

CT Manifestations of Coronavirus Disease (COVID-19) Pneumonia and Influenza Virus Pneumonia: A Comparative Study

Liaoyi Lin, MD¹, Gangze Fu, MD, Shuangli Chen, MD, Jiejie Tao, MD, Andan Qian, MD, Yunjun Yang, PhD, Meihao Wang, PhD

Cardiothoracic Imaging · Original Research

Keywords

coronavirus disease, COVID-19, CT, imaging features, infection, influenza virus, novel coronavirus, pneumonia

Submitted: Apr. 6, 2020
Revision requested: Apr. 15, 2020
Revision received: May 5, 2020
Accepted: May 13, 2020

The authors declare that they have no disclosures relevant to the subject matter of this article.

OBJECTIVE. The purpose of this study was to investigate differences in CT manifestations of coronavirus disease (COVID-19) pneumonia and those of influenza virus pneumonia.

MATERIALS AND METHODS. We conducted a retrospective study of 52 patients with COVID-19 pneumonia and 45 patients with influenza virus pneumonia. All patients had positive results for the respective viruses from nucleic acid testing and had complete clinical data and CT images. CT findings of pulmonary inflammation, CT score, and length of largest lesion were evaluated in all patients. Mean density, volume, and mass of lesions were further calculated using artificial intelligence software. CT findings and clinical data were evaluated.

RESULTS. Between the group of patients with COVID-19 pneumonia and the group of patients with influenza virus pneumonia, the largest lesion close to the pleura (i.e., no pulmonary parenchyma between the lesion and the pleura), mucoid impaction, presence of pleural effusion, and axial distribution showed statistical difference ($p < 0.05$). The properties of the largest lesion, presence of ground-glass opacity, presence of consolidation, mosaic attenuation, bronchial wall thickening, centrilobular nodules, interlobular septal thickening, crazy paving pattern, air bronchogram, unilateral or bilateral distribution, and longitudinal distribution did not show significant differences ($p > 0.05$). In addition, no significant difference was seen in CT score, length of the largest lesion, mean density, volume, or mass of the lesions between the two groups ($p > 0.05$).

CONCLUSION. Most lesions in patients with COVID-19 pneumonia were located in the peripheral zone and close to the pleura, whereas influenza virus pneumonia was more prone to show mucoid impaction and pleural effusion. However, differentiating between COVID-19 pneumonia and influenza virus pneumonia in clinical practice remains difficult.

In December 2019, an epidemic caused by severe acute respiratory syndrome coronavirus 2 (SARS-CoV-2) broke out in Wuhan, China. Coronavirus disease (COVID-19), the disease that results from SARS-CoV-2 infection, has caused human-to-human transmission and death in China and many other countries [1]. Pulmonary inflammation is the main pathologic manifestation of COVID-19. CT manifestations vary and include ground-glass opacity (GGO), consolidation, or GGO mixed with consolidation. Vascular enlargement, interlobular septal thickening, and air bronchogram are also seen. Most lesions are located in the peripheral subpleural zone, primarily in the posterior or lower lobe. Lesions may extend from the periphery to the center as they deteriorate [2–6].

Influenza is a highly contagious disease that occurs worldwide. Influenza viruses type A and occasionally type B cause influenza virus pneumonia, which results in seasonal epidemics of community-acquired pneumonia. Diffuse or patchy GGO mixed with consolidation is often seen on CT of patients with influenza virus pneumonia. Studies have found that the main CT manifestations of influenza virus pneumonia are GGO and consolidation with air bronchogram, interlobular septal thickening, centrilobular nodules, and reticular opacities [7, 8]. Some texture-based recognition systems have been developed to classify pneumonia pattern through texture differences; for instance, Yao et al. [9] used computer-aided texture analysis methods to identify and measure pulmonary abnormalities on chest CT images of patients with influenza virus pneumonia. Their results indicated that texture analysis can distinguish abnormal acute infection from chronic fibrotic lesions of consolidation and GGO and that quantifying texture features on CT

doi.org/10.2214/AJR.20.23304
AJR 2021; 216:1–9
ISSN-L 0361–803X/21/2161–1
© American Roentgen Ray Society

¹All authors: Department of Radiology, The First Affiliated Hospital of Wenzhou Medical University, Wenzhou, 325000, China. Address correspondence to M. Wang (wzwmh@wmu.edu.cn).

can allow more accurate assessment of the progression and severity of disease.

The CT manifestations of viral pneumonia are related to the pathogenesis of pulmonary viral infection, so viral pneumonias caused by similar viruses will show similar disease patterns and CT manifestations. GGO and consolidation are CT manifestations of both COVID-19 pneumonia and influenza virus pneumonia [10]. However, to our knowledge, the differences between COVID-19 pneumonia and influenza virus pneumonia have not yet been studied. We conducted this study to compare CT morphologic features and quantitative parameters of COVID-19 pneumonia and influenza virus pneumonia. In addition, artificial intelligence (AI)-assisted software was used to measure and calculate volume, mass, and mean density of inflammatory lesions to provide quantitative indicators from imaging studies. Our goal was to provide points of reference for distinguishing SARS-CoV-2 infection from influenza virus infection.

Materials and Methods

Patients

The retrospective data assessment was approved by the ethics committee, and the requirement of written informed consent was waived. We reviewed the records of consecutive patients with COVID-19 who had positive results from SARS-CoV-2 nucleic acid testing at the First and Second Affiliated Hospital of Wenzhou Medical University and Wenzhou Yueqing People's Hospital from January 17, 2020, to February 13, 2020. Inclusion criteria were absence of hypertension, diabetes, tumor, chronic obstructive pulmonary disease, bronchiectasis, lung cancer, and other lung diseases; availability of complete data from CT examinations; complete clinical data for the patient with a clear medical history; and no coinfection. A review of patients with influenza virus pneumonia (types A and B) confirmed by nucleic acid testing at the First Affiliated Hospital of Wenzhou Medical University from February 20, 2018, to February 9, 2020 was also conducted. Inclusion criteria for patients with influenza virus pneumonia were the same as those for patients with COVID-19 pneumonia.

CT

All patients underwent unenhanced CT in the supine position with breath-holding after inspiration. The scan ranged from the tip of the lung to the level of the costophrenic angle. Patients from the First Affiliated Hospital of Wenzhou Medical University were imaged using Brilliance 16 (Philips Healthcare), Somatom Scope 16 (Siemens Healthineers), or LightSpeed VCT 64 (GE Healthcare) scanners and the following parameters: tube voltage of 120 kV, tube current–exposure time product of 50–150 mAs, scan thickness of 5 mm, and reconstruction thickness of 1.25 mm. Patients from the Second Affiliated Hospital of Wenzhou Medical University were imaged using a Brilliance 16 scanner with the following parameters: tube voltage of 120 kV, tube current–exposure time product of 150 mAs, scan thickness of 5 mm, and reconstruction thickness of 5 mm. Patients from Wenzhou Yueqing People's Hospital were imaged using a Somatom Scope 16 scanner with the following parameters: tube voltage of 110–130 kV, tube current–exposure time product of 70 mAs, scan thickness of 5 mm, and reconstruction thickness of 1.5 mm.

All image data were transmitted to a PACS system after scanning was completed.

Image Evaluation

Images were reviewed by two chest radiologists, each of whom had 5 years' experience. If the radiologists initially had discordant decisions, a final decision was reached by consensus. The presence or absence of the following CT manifestations was noted: consolidation (an area of increased attenuation that obscures the vascular structure), GGO (hazy areas of increased opacity or attenuation that do not obscure the underlying vessels), centrilobular nodules (nodules located around peripheral pulmonary arterial branches or 3–5 mm away from the pleura, interlobular septa, pulmonary veins, or relatively proximal pulmonary arteries), mosaic attenuation (sharply demarcated areas of inhomogeneous attenuation in which areas of normal lung are seen between areas of GGO), bronchial wall thickening, interlobular septal thickening, mucus impaction, pleural effusion, and crazy paving pattern (a network of smooth linear patterns superimposed on an area of GGO) [11, 12]. The main CT feature, or property, of the largest lesion in each patient was characterized as GGO, consolidation, or a mixture of GGO and consolidation. Whether the largest lesion was close to the pleura (i.e., no significant amount of pulmonary parenchyma was seen between the lesion and the pleura) was recorded, as well as whether the lesion was unilateral or bilateral. The predominant axial (inner, outer, diffuse, or random) and longitudinal (upper, lower, diffuse, or random) distributions of abnormalities were determined for each patient. For axial distribution, the boundary between inner and outer distribution was set at a distance of 30 mm from the pleura. For longitudinal distribution, the upper lung zone was at a level above the tracheal carina, whereas the lower lung zone was located below the tracheal carina. Diffuse distribution was defined as lesions that were distributed across boundaries, whether axial or longitudinal; if abnormalities showed no clear zonal predominance, disease was classified as randomly distributed.

Through semiquantitative analysis, the lesion properties, distribution, and range of lung lesions were evaluated to objectively assess damage to lung tissue. The presence of GGO or consolidation of the inflammatory lesions, which could coexist or be accompanied by interlobular septal thickening, was noted. The appearance of lesions on axial CT images was assigned a score on a 3-point scale: 0, normal attenuation; 1, GGO; and 2, consolidation [13]. The affected lung parenchyma was assigned a score on a 6-point scale according to the extent of lobar involvement in each lobe: 0, none; 1, < 5%; 2, 5–25%; 3, 25–50%; 4, 50–75%; and 5, > 75%. The two scores for each region were then multiplied, and the resulting products were summed to obtain the final total cumulative CT score, which ranged from 0 to 50 [14]. The length of the largest lesion was recorded.

Inflammatory lesions seen on chest CT were analyzed with AI assistance software (FACT [pneumonia intelligent analysis model], version 1.7.0.1, Dexin Medical Imaging Technology). The software could automatically identify and delineate the areas of pneumonia lesions. After the ROI was manually adjusted, the software automatically calculated the volume and mean density of the lesions. The mass (in grams) of the lesion was calculated us-

TABLE 1: Patient Information

Characteristic	Total	COVID-19 Pneumonia	Influenza Virus Pneumonia	<i>p</i>
No. of patients	97	52	45	
Sex				0.183
Male	48	29	19	
Female	49	23	26	
Age (y)	44.86 ± 13.67	44.98 ± 11.29	44.73 ± 16.12	0.756
Duration of initial symptoms (d)	5.03 ± 3.60	4.70 ± 3.80	5.41 ± 3.36	0.132
Fever				1.000
No	13	7	6	
Yes	84	45	39	
Duration of fever (d)	4.18 ± 3.46	3.99 ± 3.56	4.41 ± 3.36	0.326

Note—Except for *p* values, data are either number of patients or mean ± SD. COVID-19 = coronavirus disease.

ing the formula: volume (in cubic centimeters) × (attenuation [in Hounsfield units] + 1000) / 1000 [15].

Statistical Analysis

SPSS software (version 24.0, IBM) was used to process the data. Continuous variables were expressed as means ± SD, and categorical variables were expressed as numbers. The Fisher exact test and the chi-square test were used for categorical variables, and the Mann-Whitney *U* test was used for continuous variables. Any *p* value less than 0.05 was considered statistically significant.

Results

Patient Information

A total of 97 patients (49 women, 48 men; mean age ± SD, 44.86 ± 13.67 years) were enrolled in this study. Of them, 52 patients (29 men, 23 women; mean age, 44.98 ± 11.28 years; age range, 21–73 years) had COVID-19 pneumonia; 45 patients (26 women, 19 men; mean age, 44.73 ± 16.12 years; age range, 15–76 years) had influenza virus pneumonia (28, influenza A; 17, influenza B). No significant differences were seen in sex, age, duration of initial symptoms, fever, or duration of fever between patients with COVID-19 pneumonia and those with influenza virus pneumonia (*p* > 0.05) (Table 1). The initial symptoms for patients with COVID-19 were fever (*n* = 35), cough (*n* = 9), sore throat (*n* = 1), gastrointestinal symptoms (*n* = 2), debilitation or myalgia (*n* = 2), and no obvious symptoms (*n* = 3). For patients with influenza, the initial symptoms were fever (*n* = 14), fever with cough or sore throat (*n* = 23), and cough or sore throat (*n* = 8).

CT Imaging Comparison

In patients with COVID-19 pneumonia, the most common main CT feature of the largest lesion was GGO (30/52, 57.7%). The largest lesions were close to the pleura in 36 cases (69.2%) (Fig. 1). GGO was seen in 44 patients (84.6%), consolidation in 28 (53.8%), and mosaic attenuation in 10 (19.2%). Six patients (11.5%) had bronchial wall thickening, 12 (23.1%) had centrilobular nodules, 14 (26.9%) had interlobular septal thickening, seven (13.5%) had crazy paving pattern, 18 (34.6%) had air bronchogram, one (1.9%) had mucoid impaction, and no patient had obvious pleural effusion.

In patients with influenza virus pneumonia, the most common main CT feature of the largest lesion was also GGO (21/45, 46.7%). The largest lesions were close to the pleura in 18 cases (40%), but most lesions were not close to the pleura (Fig. 2). GGO was seen in 32 patients (71.1%), consolidation was seen in 26 (57.8%), and mosaic attenuation was seen in 10 (22.2%). Seven patients (15.6%) had bronchial wall thickening, five (11.1%) had centrilobular nodules, 10 (22.2%) had interlobular septal thickening, six (13.3%) had crazy paving pattern, 17 (37.8%) had air bronchogram, six (13.3%) had mucoid impaction (Fig. 3), and 10 (22.2%) had pleural effusion (Fig. 4).

With regard to lesion distribution, in patients with COVID-19 pneumonia, unilateral lung lesion distribution was seen in 14 (26.9%); lesions were distributed bilaterally in 38 patients (73.1%). For axial distribution, lesions were located in the outer zone in 35 patients (67.3%). For longitudinal distribution, lesions were located in the lower zone (Fig. 5) in 32 patients (61.5%). Of the patients with influenza virus pneumonia, 20 (44.4%) had unilateral lesion distribution, and 25 (55.6%) had bilateral lesion distribution. The axial distribution of lesions was diffuse in 16 patients (35.6%) and random in 15 (33.3%). With respect to longitudinal distribution, lesions were located in the lower zone (Fig. 6) in 32 patients (71.1%).

Statistically significant differences were seen between the two types of pneumonia with respect to whether the largest lesion was close to the pleura, presence of mucoid impaction, presence of pleural effusion, and axial distribution (*p* < 0.05). However, no significant difference was seen in the properties of the largest lesion, presence of GGO, presence of consolidation, presence of mosaic attenuation, bronchial wall thickening, centrilobular nodules, interlobular septal thickening, crazy paving pattern, air bronchogram, laterality, or longitudinal distribution (*p* > 0.05). Further analysis of the severity of the lesions revealed no significant differences in CT score, length of the largest lesion, mean density, volume, or mass of lesions between the two patient groups (*p* > 0.05) (Table 2).

Discussion

SARS-CoV-2, the seventh member of the coronavirus family to infect humans, can spread from human to human. It poses a seri-

TABLE 2: Comparison of CT Findings in Patients With Coronavirus Disease (COVID-19) Pneumonia and With Influenza Virus Pneumonia

Characteristic	Total	COVID-19 Pneumonia	Influenza Virus Pneumonia	<i>p</i>
No. of patients	97	52	45	
Properties of largest lesion				0.470
GGO	51	30	21	
Consolidation	41	19	22	
Mixed GGO and consolidation	5	3	2	
Length (mm)	35.18 ± 26.09	34.28 ± 23.10	36.20 ± 29.41	0.825
Lesions close to the pleura				0.005
No	43	16	27	
Yes	54	36	18	
GGO				0.140
No	21	8	13	
Yes	76	44	32	
Consolidation				0.838
No	43	24	19	
Yes	54	28	26	
Mosaic attenuation				0.803
No	77	42	35	
Yes	20	10	10	
Bronchial wall thickening				0.766
No	84	46	38	
Yes	13	6	7	
Centrilobular nodules				0.181
No	80	40	40	
Yes	17	12	5	
Interlobular septal thickening				0.593
No	73	38	35	
Yes	24	14	10	
Crazy paving pattern				1.000
No	84	45	39	
Yes	13	7	6	
Mucoid impaction				0.047
No	90	51	39	
Yes	7	1	6	
Pleural effusion				< 0.001
No	87	52	35	
Yes	10	0	10	
Air bronchogram				0.833
No	62	34	28	
Yes	35	18	17	
Lesion laterality				0.089
Unilateral	34	14	20	
Bilateral	63	38	25	

(Table 2 continues on next page)

TABLE 2: Comparison of CT Findings in Patients With Coronavirus Disease (COVID-19) Pneumonia and With Influenza Virus Pneumonia (continued)

Characteristic	Total	COVID-19 Pneumonia	Influenza Virus Pneumonia	<i>p</i>
Axial distribution				< 0.001
Inner	6	3	3	
Outer	46	35	11	
Diffuse	22	6	16	
Random	23	8	15	
Longitudinal distribution				0.588
Upper	5	4	1	
Lower	64	32	32	
Diffuse	10	6	4	
Random	18	10	8	
CT score	6.71 ± 6.26	6.38 ± 5.19	7.09 ± 7.36	0.819
Attenuation (HU)	-427.1 ± 134.26	-449.07 ± 107.49	-401.76 ± 157.19	0.099
Volume (cm ³)	111.08 ± 197.24	84.75 ± 125.07	141.50 ± 254.92	0.948
Mass (g)	77.47 ± 157.36	51.31 ± 87.00	107.70 ± 208.59	0.994

Note—Except for *p* values, data are either number of patients or mean ± SD. COVID-19 = coronavirus disease, GGO = ground-glass opacity.

ous public health threat [16]. Because viral pneumonia can result from infection with SARS-CoV-2 and from infection with an influenza virus, we undertook to determine if there are differences in the pneumonias caused by the different viruses. We found that the axial distribution of COVID-19 pneumonia was most often in the peripheral zone (67.3%), and the most important characteristic was that the largest lesion was close to the pleura (69.2%). Lesions from influenza virus pneumonia had more diffuse (35.6%) or random (33.3%) distribution, and the largest lesion was close to the pleura (40%) less often than was seen in patients with COVID-19 pneumonia. These results are consistent with those of previous studies. In a study of 21 patients with COVID-19 pneumonia, Chung et al. [2] noted a large number of areas of GGO and consolidation on chest CT, which were distributed in the peripheral pulmonary zone. Song et al. [17] studied CT findings of 51 patients with COVID-19 pneumonia and found that 44 patients (86%) were affected in peripheral lung, suggesting that peripheral distribution is a characteristic of COVID-19 pneumonia.

We also focused on lesion distribution and found that an important characteristic of COVID-19 pneumonia was that lesions were close to the pleura, that is, without pulmonary parenchyma between the lesion and the pleura. In patients with influenza virus pneumonia, by contrast, the axial distribution was more often diffuse or random (68.9%). In a study by Tanaka et al. [12] of the CT manifestations of the influenza virus pneumonia, diffuse and random axial distributions were commonly seen, which is consistent with our findings. The difference in the axial distributions of lesions in the two viral pneumonias suggests that COVID-19 pneumonia might originate from the subpleural mesenchyme and gradually spread inward.

Another important finding of our study was that influenza virus pneumonia showed more mucus impaction (13.3%) and pleural effusion (22.2%) than did COVID-19 pneumonia, which showed only one case of mucus impaction and no significant pleural effu-

sion. Lesions from influenza virus pneumonia appeared to have more mucous composition and pleural effusion, perhaps because the influenza virus tends to affect large and small airways and lung parenchyma, leading to excessive mucus production [18]. Bacteria, viruses, or fungi infecting pleura can cause infective inflammation and generate pleural effusion, and although pleural effusion in viral pneumonia is relatively rare, influenza virus pneumonia with pleural effusion has been reported in previous studies, possibly reflecting secondary bacterial infection or progression of disease [19, 20]. None of our patients with influenza virus pneumonia had clear evidence of bacterial infection. Xu et al. [21] found that pleural effusion was rare in patients with COVID-19 pneumonia, which is consistent with our findings [21].

We found no significant differences between the two viral pneumonias in terms of the properties of the largest lesion, presence of GGO, presence of consolidation, presence of mosaic attenuation, bronchial wall thickening, centrilobular nodules, interlobular septal thickening, crazy paving pattern, air bronchogram, unilateral or bilateral distribution, or longitudinal distribution of lesions. This outcome may be related to the fact that viral pneumonias have similar pathogenetic patterns, so imaging signs of different viral pneumonias will overlap. Histologic findings of rapidly progressive pneumonia include transparent membrane formation and diffuse alveolar damage, including interstitial lymphocyte infiltration, air-space hemorrhage, edema, fibrin, and type II cell proliferation [22]. CT findings of pneumonia are similar and include centrilobular nodules, GGO with lobular distribution, segmental consolidation, or diffuse GGO with interlobular septal thickening [23]. In a study of 41 patients with COVID-19 pneumonia, 40 patients had hazy opacities in both sides of the lung on chest CT with the most typical manifestations being lobular and subsegmental consolidation [24]. Reported CT manifestations of influenza virus pneumonia include GGO, patchy consolidation, centrilobular nodules, and tree-in-bud pattern [25]. Kim et al. [22] evaluated CT findings of influ-

enza virus pneumonia and found multifocal peribronchovascular or bilateral subpleural consolidation with GGO. GGO and consolidation were common on CT images of viral pneumonia and were associated with diffuse alveolar damage. Crazy paving pattern and mosaic attenuation have also been reported to be common CT findings in cases of diffuse alveolar damage [26, 27]. However, in our study, the difference in frequency of these two characteristics was not statistically significant between the two patient groups. Similarly, we did not find a significant difference in the presence of GGO and consolidation lesions between the two types of viral pneumonia. In addition, the CT images of pneumonia lesions were quantitatively analyzed using AI software. Finally, we obtained the CT score, length of the largest lesion, mean density, volume, and mass of the lesions. We found no significant differences in any of these characteristics, which indicates a high degree of overlap in the CT manifestations of the two types of pneumonia.

The CT score, mean density, and mass of lesions in patients with CT consolidation showed a more severe clinical course of viral pneumonia in those patients compared with patients with GGO [28]. The CT score, length of the largest lesion, and lesion volume reflect the range of lesion involvement, so larger lesions corresponded with higher quantitative parameters. We found no significant difference in duration of initial symptoms and duration of fever, and the courses of disease were similar. Although there were no significant differences, the CT score, length of the largest lesions, mean density, volume, and mass for influenza virus pneumonia lesions were slightly higher than for lesions from COVID-19 pneumonia, which suggests that influenza virus pneumonia is more serious in the early stages of the disease.

Our study has several limitations. First, it was retrospective. Because of the timing of the outbreak of SARS-CoV-2, the collection of patients with COVID-19 pneumonia was concentrated in January and February 2020, whereas the collection of patients with influenza virus pneumonia patients took place over a longer period of time from 2018 to 2020. Thus, selection bias could not be completely avoided. Second, data from patients with COVID-19 pneumonia were obtained from multiple institutions that use different scanning parameters, so some patients were scanned with different section thicknesses (1.5 mm versus 5 mm), and subtle structures such as centrilobular nodules may have been hidden or overlooked in some instances.

In conclusion, our study found that most lesions from COVID-19 pneumonia were located in the peripheral zone and close to the pleura, whereas lesions from influenza virus pneumonia were diffuse or in random distribution and further from the pleura. Mucoid impaction and pleural effusion were more prone to occur with influenza virus pneumonia than with COVID-19 pneumonia. Those signs should be noted when assessing patients with pneumonia to determine whether the cause is COVID-19 or influenza. However, CT manifestations of COVID-19 pneumonia and influenza virus pneumonia have a large amount of overlap, such that even with the characteristics evaluated using AI software, no significant differences were detected. Distinguishing between these two types of viral pneumonia with imaging alone is difficult. Therefore, CT examination needs to be combined with clinical indicators for comprehensive evaluation; the more important role of CT in the pandemic is in finding lesions and evaluating effects of treatment.

References

- Li Q, Guan X, Wu P, et al. Early transmission dynamics in Wuhan, China, of novel coronavirus-infected pneumonia. *N Engl J Med* 2020; 382:1199–1207
- Chung M, Bernheim A, Mei X, et al. CT imaging features of 2019 novel coronavirus (2019-nCoV). *Radiology* 2020; 295:202–207
- Li Y, Xia L. Coronavirus disease 2019 (COVID-19): role of chest CT in diagnosis and management. *AJR* 2020; 214:1280–1286
- Zhao W, Zhong Z, Xie X, Yu Q, Liu J. Relation between chest CT findings and clinical conditions of coronavirus disease (COVID-19) pneumonia: a multicenter study. *AJR* 2020; 214:1072–1077
- Zu ZY, Jiang MD, Xu PP, Chen W, Ni QQ. Coronavirus disease 2019 (COVID-19): a perspective from China. *Radiology* 2020 Feb 21 [Epub ahead of print]
- Zhou S, Wang Y, Zhu T, Xia L. CT features of coronavirus disease 2019 (COVID-19) pneumonia in 62 patients in Wuhan, China. *AJR* 2020; 214:1287–1294
- Wang Q, Zhang Z, Shi Y, Jiang Y. Emerging H7N9 influenza A (novel reassortant avian-origin) pneumonia: radiologic findings. *Radiology* 2013; 268:882–889
- Yuan Y, Tao XF, Shi YX, Liu SY, Chen JQ. Initial HRCT findings of novel influenza A (H1N1) infection. *Influenza Other Respir Viruses* 2012; 6:e114–e119
- Yao J, Dwyer A, Summers RM, Mollura DJ. Computer-aided diagnosis of pulmonary infections using texture analysis and support vector machine classification. *Acad Radiol* 2011; 18:306–314
- Xu YH, Dong JH, An WM, et al. Clinical and computed tomographic imaging features of novel coronavirus pneumonia caused by SARS-CoV-2. *J Infect* 2020; 80:394–400
- Omeri AK, Okada F, Takata S, et al. Comparison of high-resolution computed tomography findings between *Pseudomonas aeruginosa* pneumonia and cytomegalovirus pneumonia. *Eur Radiol* 2014; 24:3251–3259
- Tanaka N, Emoto T, Suda H, et al. High-resolution computed tomography findings of influenza virus pneumonia: a comparative study between seasonal and novel (H1N1) influenza virus pneumonia. *Jpn J Radiol* 2012; 30:154–161
- Feng F, Jiang Y, Yuan M, et al. Association of radiologic findings with mortality in patients with avian influenza H7N9 pneumonia. *PLoS One* 2014; 9:e93885
- Chang YC, Yu CJ, Chang SC, et al. Pulmonary sequelae in convalescent patients after severe acute respiratory syndrome: evaluation with thin-section CT. *Radiology* 2005; 236:1067–1075
- Mull RT. Mass estimates by computed tomography: physical density from CT numbers. *AJR* 1984; 143:1101–1104
- Zhu N, Zhang D, Wang W, et al.; China Novel Coronavirus Investigating and Research Team. A novel coronavirus from patients with pneumonia in China, 2019. *N Engl J Med* 2020; 382:727–733
- Song F, Shi N, Shan F, et al. Emerging 2019 novel coronavirus (2019-nCoV) pneumonia. *Radiology* 2020; 295:210–217
- Deng J, Zheng Y, Li C, Ma Z, Wang H, Rubin BK. Plastic bronchitis in three children associated with 2009 influenza A (H1N1) virus infection. *Chest* 2010; 138:1486–1488
- Kim YN, Cho HJ, Cho YK, Ma JS. Clinical significance of pleural effusion in the new influenza A (H1N1) viral pneumonia in children and adolescent. *Pediatr Pulmonol* 2012; 47:505–509
- Zheng Y, He Y, Deng J, et al. Hospitalized children with 2009 influenza A (H1N1) infection in Shenzhen, China, November–December 2009. *Pediatr Pulmonol* 2011; 46:246–252
- Xu X, Yu C, Qu J, et al. Imaging and clinical features of patients with 2019 novel coronavirus SARS-CoV-2. *Eur J Nucl Med Mol Imaging* 2020; 47:1275–1280
- Kim EA, Lee KS, Primack SL, et al. Viral pneumonias in adults: radiologic and pathologic findings. *RadioGraphics* 2002; 22:S137–S149

23. Koo HJ, Lim S, Choe J, Choi SH, Sung H, Do KH. Radiographic and CT features of viral pneumonia. *RadioGraphics* 2018; 38:719–739
24. Huang C, Wang Y, Li X, et al. Clinical features of patients infected with 2019 novel coronavirus in Wuhan, China. *Lancet* 2020; 395:497–506
25. Oikonomou A, Müller NL, Nantel S. Radiographic and high-resolution CT findings of influenza virus pneumonia in patients with hematologic malignancies. *AJR* 2003; 181:507–511
26. Johkoh T, Itoh H, Müller NL, et al. Crazy-paving appearance at thin-section CT: spectrum of disease and pathologic findings. *Radiology* 1999; 211:155–160
27. Ichikado K, Suga M, Gushima Y, et al. Hyperoxia-induced diffuse alveolar damage in pigs: correlation between thin-section CT and histopathologic findings. *Radiology* 2000; 216:531–538
28. Grinblat L, Shulman H, Glickman A, Matukas L, Paul N. Severe acute respiratory syndrome: radiographic review of 40 probable cases in Toronto, Canada. *Radiology* 2003; 228:802–809

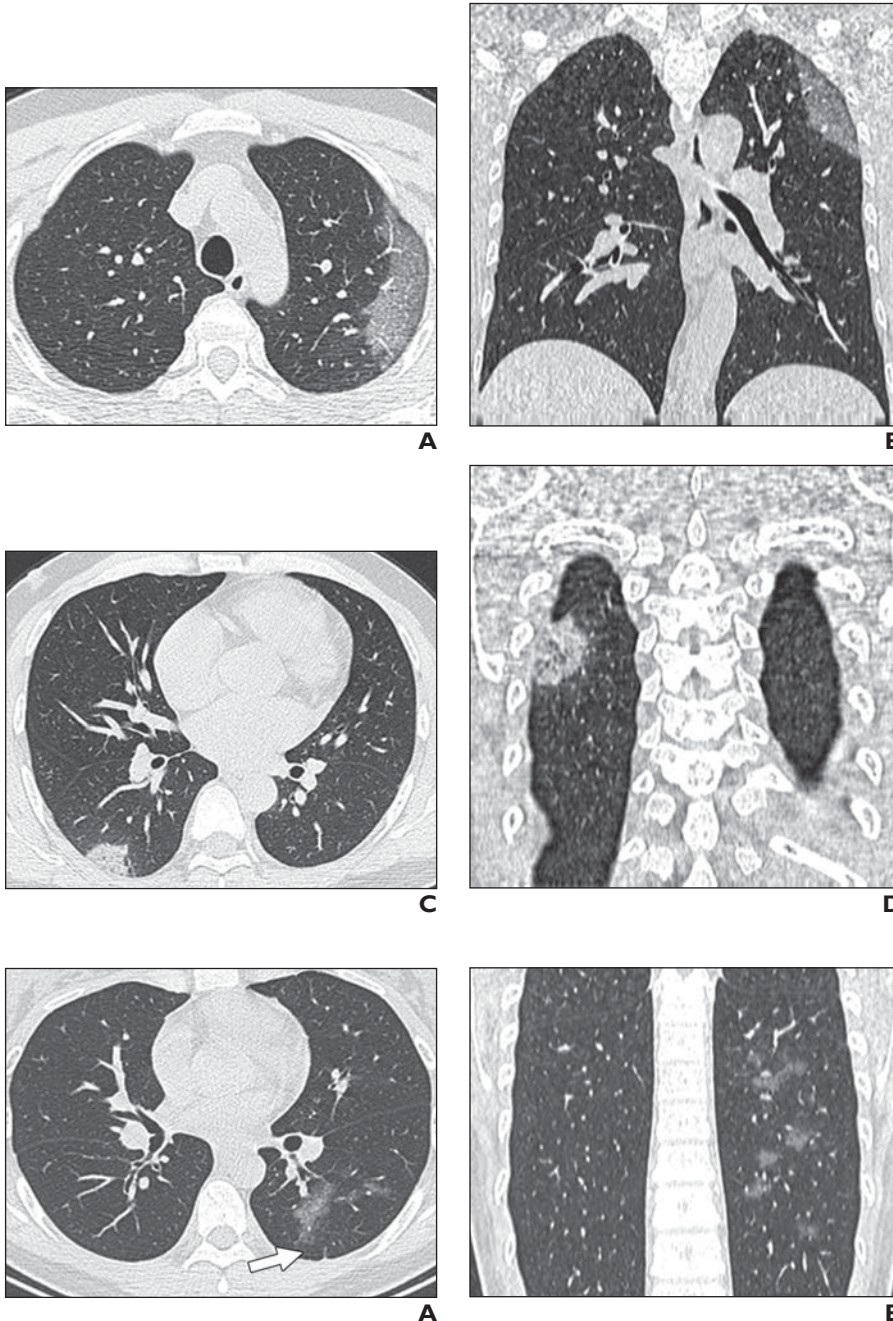


Fig. 1—41-year-old man with coronavirus disease (COVID-19) pneumonia who had experienced diarrhea for 1 week and fever for 3 days. **A** and **B**, Transverse (**A**) and coronal (**B**) CT images show ground-glass opacity, lesion close to pleura, interlobular septal thickening under ground-glass opacity, and crazy paving pattern in left upper lung. **C** and **D**, Transverse (**C**) and coronal (**D**) CT images show small area of consolidation in right lower lung, air bronchogram, and lesion close to pleura.

Fig. 2—31-year-old woman with influenza virus pneumonia who had experienced fever and cough for 4 days. **A**, Transverse CT image shows that left lower lung had ground-glass opacity, and lesion (*arrow*) is not close to pleura. **B**, Coronal CT image shows that most areas of ground-glass opacity are located away from pleura.

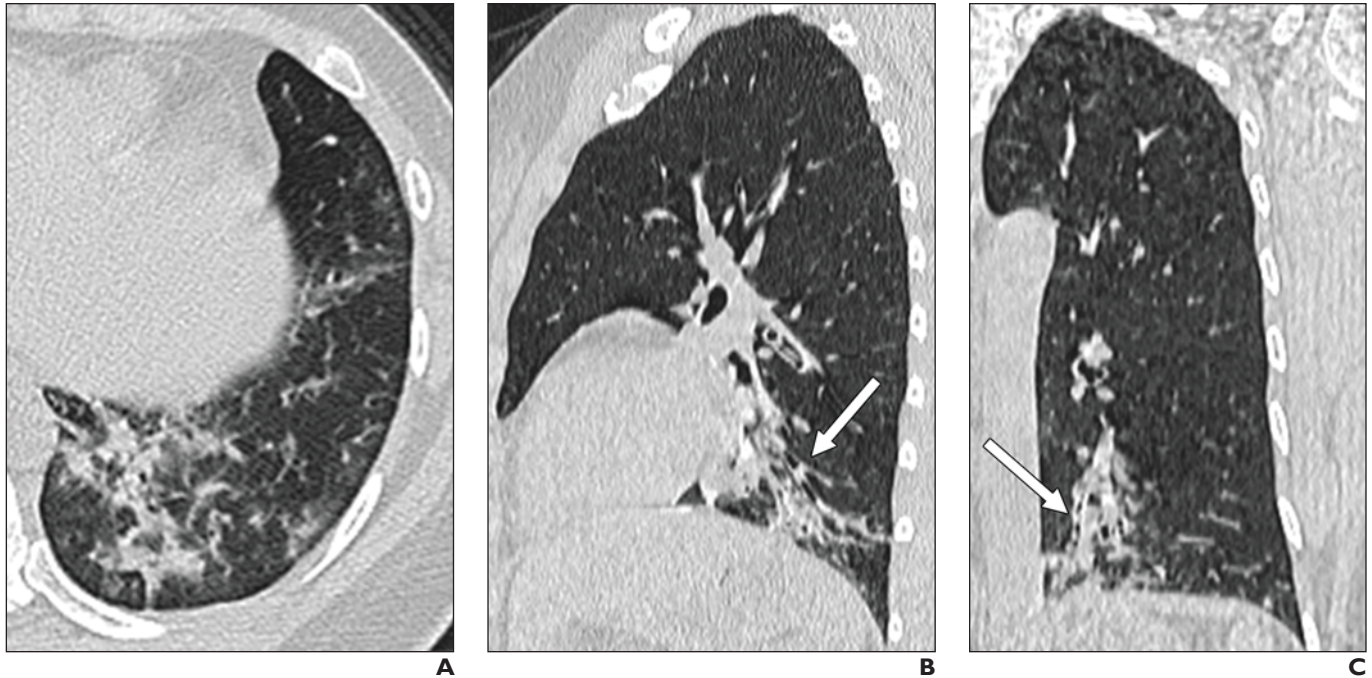


Fig. 3—32-year-old woman with influenza virus pneumonia who had experienced fever, cough, and expectoration for 5 days. **A**, Transverse CT image shows patchy consolidation in left lower lung and scattered ground-glass opacity with parenchyma between lesion and pleura. **B** and **C**, Sagittal (**B**) and coronal (**C**) images show local bronchial mucoid impaction (*arrow*) in left lower lung.

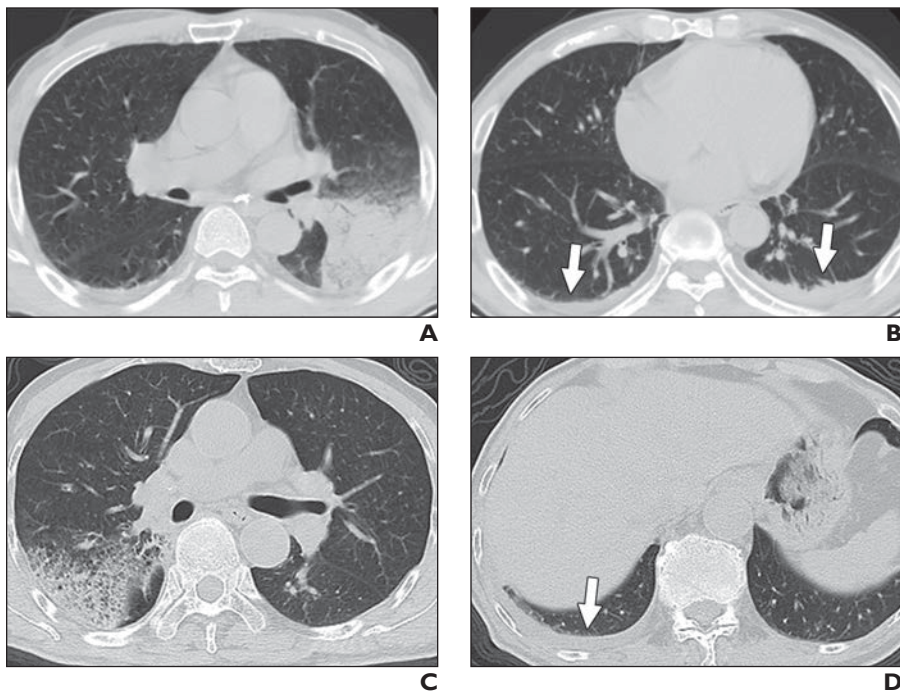


Fig. 4—Two patients with influenza virus pneumonia who had pleural effusion. In our study, influenza virus pneumonia was more likely to show pleural effusion. **A** and **B**, 51-year-old man with fever for 5 days. Axial CT image at level of pulmonary artery trunk (**A**) shows consolidation in left lower lung. Axial CT image at level of left ventricle (**B**) shows pleural effusion in bilateral thorax (*arrows*). **C** and **D**, 74-year-old man with fever and cough for 10 days. Axial CT image at level of pulmonary artery trunk (**C**) shows patchy consolidation in right upper lung. Axial CT image at level of T11 (**D**) shows pleural effusion in right thorax (*arrow*).

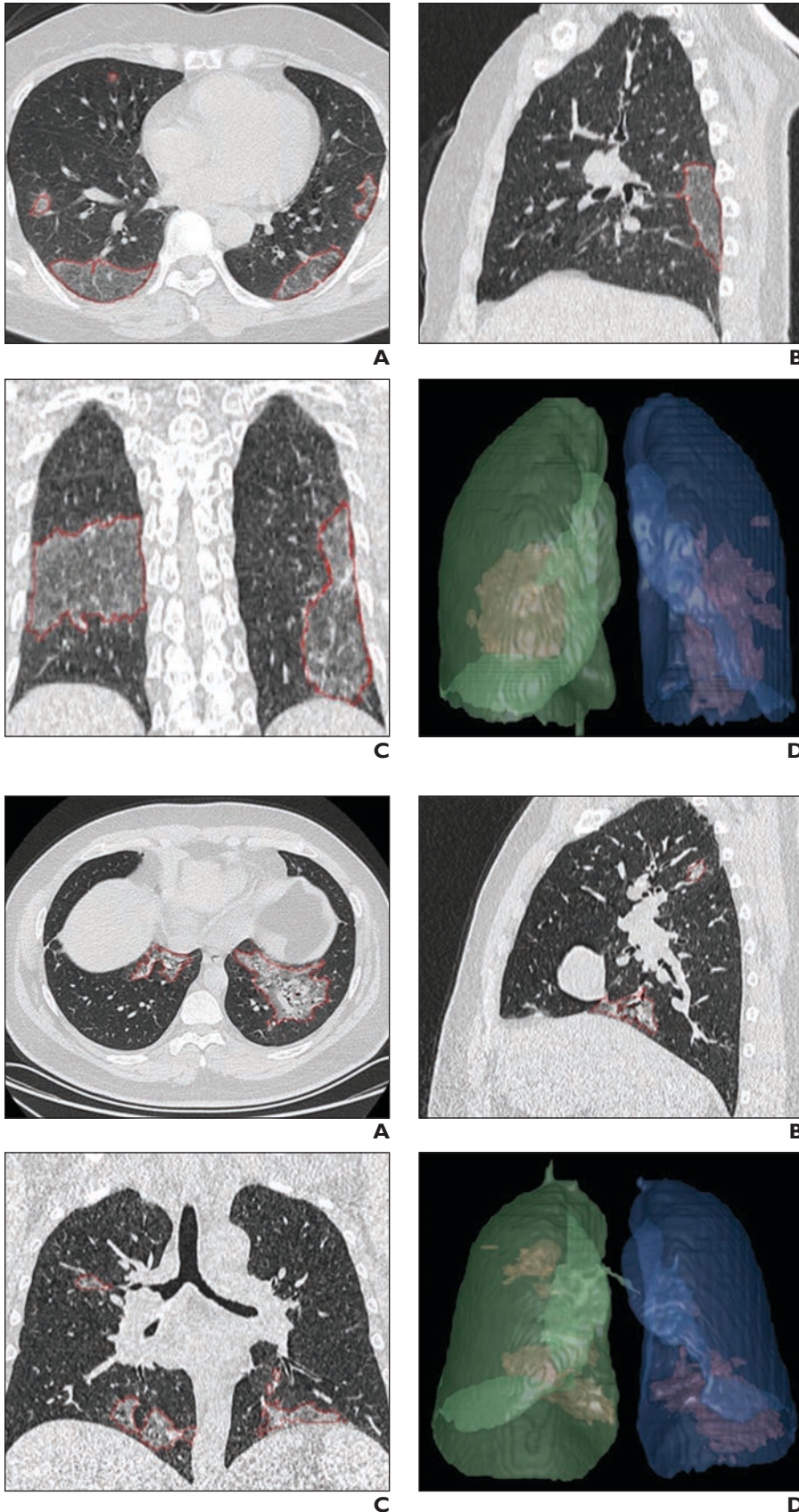


Fig. 5—57-year-old woman with coronavirus disease (COVID-19) pneumonia and fever for 6 days. Artificial intelligence (AI)-assisted software was used to identify inflammatory tissues in lung and automatically segment inflammatory lesions. Software imposed red boundaries seen in **A–C** as part of visualization processing.
A, Transverse CT image shows that main lesion is ground-glass opacity located in bilateral lower lobes of lung, axial distribution is peripheral, and largest lesion is close to pleura.
B and **C**, Sagittal (**B**) and coronal (**C**) CT images show that longitudinal distribution of lesions was in lower zone. Lesions are still close to pleura.
D, Three-dimensional image shows regions of COVID-19 pneumonia in lung through AI postprocessing.

Fig. 6—34-year-old man with influenza virus pneumonia and fever for 2 days. Artificial intelligence (AI)-assisted software was used to automatically segment inflammatory lesions. Software imposed red boundaries seen in **A–C** as part of visualization processing.
A, Transverse CT image shows that main lesion is mixed consolidation and ground-glass opacity in left lower lobe of lung, and axial distribution is diffuse.
B and **C**, Sagittal (**B**) and coronal (**C**) images show that lesions were mainly located under tracheal carina (i.e., longitudinal distribution was in lower zone).
D, Three-dimensional image shows regions of influenza virus pneumonia in lung through AI postprocessing.